Robles Martínez, Á.; Capson-Tojo, G.; Gales, A.; Ruano, MV.; Sialve, B.; Ferrer, J.; Steyer, J. (2020). Microalgae-bacteria consortia in high-rate ponds for treating urban wastewater: Elucidating the key state indicators under dynamic conditions. Journal of Environmental Management. 261:1-11. https://doi.org/10.1016/j.jenvman.2020.110244

Microalgae-bacteria consortia in high-rate ponds for treating urban wastewater: elucidating the key state indicators under dynamic conditions

Ángel Robles [a,*], Gabriel Capson-Tojo [b], Amandine Galès [c], María Victoria Ruano [a], Bruno Sialve [c], José Ferrer [d], Jean-Philippe Steyer [c]

[a] Departament d'Enginyeria Química, Escola Tècnica Superior D'Enginyeria, Universitat de València, Avinguda de la Universitat s/n, 46100, Burjassot, Valencia, Spain

[b] CRETUS Institute, Department of Chemical Engineering, School of Engineering, Universidade de Santiago de Compostela, 15782, Santiago de Compostela, Spain

[c] LBE, Univ. Montpellier, INRA, 102 avenue des Etangs, 11100, Narbonne, France

[d] Institut Universitari d'Investigació d'Enginyeria de l'Aigua i Medi Ambient (IIAMA), Universitat Politècnica de València, Camí de Vera s/n, 46022, Valencia, Spain

[*] Corresponding author: tel. +34 96 354 30 85, e-mail: *angel.robles@uv.es*

Abstract

On-line performance indicators of a microalgae-bacteria consortium were screened out from different variables based on pH and dissolved oxygen on-line measurements via multivariate projection analysis, aiming at finding on-line key state indicators to easily monitor the process. To fulfil this objective, a pilot-scale high-rate pond for urban wastewater treatment was evaluated under highly variable conditions, *i.e.* during the start-up period. The system was started-up without seed of either bacterial or microalgal biomass. It took around 19 days to fully develop a microalgal community assimilating nutrients significantly. Slight increases in the biomass productivities in days 26-30 suggest that the minimum time for establishing a performant bacteria-microalgae consortium could be of around one month for non-inoculated systems. At this point the process was fully functional, meeting the European discharge limits for protected areas. The results of the statistical analyses show that both the pH and the dissolved oxygen concentration represent accurately the biochemical processes taking place under the start-up of the process. Both pH and dissolved oxygen represented accurately also the performance of the high-rate algal pond, being affordable, easily-implemented, options for monitoring, control and optimize industrial-scale processes.

Keywords

Open ponds; domestic wastewater; monitoring; single-stage treatment

1. Introduction

Although it is generally accepted that the existing wastewater treatment (WWT) technology is a remarkable human achievement, modern times call for the development of novel processes, able to cope with the necessities of a modern society. The development of the so-called water resource recovery facilities (WRRFs) is moving in this direction, aiming at recovering all the valuables that are contained within wastewaters (*e.g.* reclaimed water, carbon and nutrients). Autotrophic microalgae can play a major role in WRRFs. Microalgae are photosynthetic microorganisms able to grow using inorganic carbon (*i.e.* CO_2 and HCO_3^-) as carbon source, gathering the required energy for growth and metabolism from sunlight. In addition, microalgae need macronutrients (nitrogen and phosphorous), which are consumed in their soluble inorganic forms, namely ammonium (NH_4^+) and phosphate (PO_4^{3-}). In this process, microalgal biomass is produced, together with a variety of organic compounds that are precursors of different forms of bio-energy (*e.g.* biomass itself, biodiesel, bio-ethanol and bio-butanol) and other value-added products (*e.g.* proteins) (Wang et al., 2016).

The application of microalgae-based systems in WRRFs for nutrient uptake has attracted the interest of the scientific community in the last years and several different applications can be found in the literature, such as industrial WWT (Mohd Udaiyappan et al., 2017), treatment of anaerobic digestion effluents (González-Camejo et al., 2017; Uggetti et al., 2014; Viruela et al., 2018) or integration with membrane units (Luo et al., 2017). This increased attention has occurred, not only due to the development of more sustainable WWT processes, but also due to the possibility of reducing the cost of microalgae production, which has been reported to be around $20–$200 per kg (Wang et al., 2016). The reduced carbon footprint of the WWT

process thanks to carbon dioxide biofixation by microalgae is another major advantage of microalgae-based processes (Lardon et al., 2009; Mata et al., 2010).

High rate algal ponds (HRAPs) and closed photobioreactors (PBRs) are the most commonly used technologies for microalgae cultivation (Vasumathi et al., 2012). Although higher biomass productivities have been reported using PBRs when compared with HRAPs (Ugwu et al., 2008), the latter present different advantages when dealing with wastewater-based microalgae cultivation: (i) smaller investment and operational costs, (ii) easier operation and maintenance, (iii) lower specific energy demand, (iv) natural selection of the most productive algae and (v) lower carbon and environmental footprint. Because of these reasons, HRAPs have been widely implemented for large-scale microalgae cultivation worldwide (Craggs et al., 2011; Kumar et al., 2015). Moreover, commercial production rates in HRAPs up to 40 g dry weight$\cdot m^{-2} \cdot d^{-1}$ have been reported, which represent acceptable values for an industrial process for microalgae cultivation (Dalrymple et al., 2013).

However, although microalgae cultivated in wastewater have been reported to reduce the concentrations of nutrients to very low values (*e.g.* 2.20 mg$\cdot L^{-1}$ and 0.15 mg$\cdot L^{-1}$ for NH_4-N and PO_4-P respectively), these photosynthetic organisms are not able to assimilate the high organic matter contents present in many waste streams, such as urban wastewater (UWW) (Boelee et al., 2011). Therefore, the treatment of wastewaters with high chemical oxygen demand (COD) concentrations via microalgae-based systems is frequently combined with anaerobic pretreatments or with wastewater dilution (Wang et al., 2015). One solution to this issue is the application of microalgae-bacteria consortia for WWT. In these systems, a synergy occurs that favors the growth of both algae and bacteria (Galès et al., 2019; Wang et al., 2016): while bacteria remove the input COD via heterotrophic growth (producing carbon dioxide), microalgae assimilate the nutrients and the carbon dioxide generated by the bacteria, supplying at the same time the oxygen that bacteria need. Furthermore, other advantages have

been postulated when compared to traditional microalgal cultures: (i) both algae and bacteria can supply vitamins and other compounds beneficial for the respective partner, (ii) the extracellular matrix generated by some microalgae can provide attachment sites for bacteria and act as organic carbon source, (iii) bacteria are known to favor the flocculation of algae, increasing the floc size and favoring biomass harvesting and (iv) a clear decrease in the spatial distance for oxygen and carbon dioxide exchange exists (Wang et al., 2016).

Recent studies have been carried out to demonstrate the feasibility of applying algae-bacteria consortia for WWT. Novoveská et al. (2016) carried out a long-term study using offshore PBRs for UWW treatment. They efficiently removed the nutrients via microalgal uptake, achieving removals of 75 % of total nitrogen (N_T) and 93 % of total phosphorus (P_T). At the same time, the aeration of the reactors by the photosynthetically produced oxygen supported bacterial growth, removing 92 % of the biological chemical demand (BOD) present in the influent. They also reached biomass productivities of 3.5-23 $g \cdot m^{-2} \cdot day^{-1}$ during continuous operation, with the productivity being mainly driven by temperature (T) and harvesting frequency. More recently, Foladori et al. (2018) used photo-sequencing batch reactors to treat UWW, reaching removal efficiencies of 87 % of the chemical oxygen demand (COD) and 98 % of the total Kjeldahl nitrogen (TKN). Again, the oxygen from photosynthesis was sufficient for supporting bacterial growth and thus avoid the need of external aeration.

The performance of HRAPs for WWT depends on several factors, such as light intensity, light mitigation (related mainly to the pond depth), mixing intensity, pH (usually around 7-9), T, dissolved oxygen (DO), salinity and carbon dioxide and nutrient concentrations (Faried et al., 2017; Kumar et al., 2015; Larsdotter, 2006; Park et al., 2011). Therefore, if productivities are to be improved and stable processes are to be achieved, the aforementioned parameters must be monitored and controlled (if possible), together with the most relevant process outputs, such as biomass productivity, nutrient removal rate, photosynthetic efficiency or solar-to-

biomass conversion efficiency (Havlik et al., 2013). In large-scale processes, this monitoring requires reliable sensors for on-line, in situ measurement of both physicochemical and biological process variables. Because of this, long-term studies of HRAPs for nutrient recovery from wastewater are generally fully monitored, measuring on-line the influent flow-rate, solar radiation, T, DO and pH. Among the different off-line measurements that are generally applied, the most relevant are the concentrations of suspended solids (SS), COD, N_T and P_T (Arbib et al., 2013; Fernández et al., 2016; Solimeno et al., 2017a; Tran et al., 2014). Real-time monitoring also serves for optimization and control of WWT processes. By coupling monitoring to different modelling and control approaches, several studies have shown improved performances. Relevant examples are: the optimization of the dilution rate to maximize the microalgal biomass production in PBRs (De Andrade et al., 2016); advanced control strategies for pH control to reduce CO_2 losses in tubular PBRs (Berenguel et al., 2004); model-driven optimization of the biomass production in HRAPs via closed-loop control of the operational variables (*e.g.* T, pH, or nutrient feeding rate) (Muñoz-Tamayo et al., 2013); mathematical modelling of sunlight incidence and light distribution in PBRs for optimization of the biomass production (De Andrade et al., 2016); or application of Internet of Things for monitoring and control of a microalgae cultivation coupled with a decision support system (Esposito et al., 2017). Together with an efficient monitoring of the process variables, novel models have the potential of allowing the prediction of the microalgae production rates, serving also for optimizing the operation in microalgae-bacteria consortia cultivated in HRAPs (Solimeno et al., 2017b).

The first step to achieve a proper monitoring of HRAPs treating wastewater using microalga-bacteria consortia is the selection of the most relevant variables affecting the process, which will serve as key state indicators. In addition, as the long and failure-prone start-up period in HRAPs is one of main challenges in microalgae-bacteria consortia for WWT, a proper

monitoring of this period is crucial to achieve an efficient and stable process (Liu et al., 2017). It must be mentioned that, although this has been widely researched in microalgae cultures, the results cannot be directly extrapolated to microalga-bacteria mixed systems, mainly because in the latter no external carbon dioxide is generally supplied. Addition of carbon dioxide into algae-based HRAPs for WWT has been used, not only for improving the algal growth (Craggs et al., 2011), but also for preventing free ammonia inhibition (Park et al., 2011) and for pH control in long-term studies (González-Camejo et al., 2019; Novoveská et al., 2016; Tran et al., 2014). Therefore, not adding carbon dioxide into a HRAP implies that the sole mechanisms controlling the pH of the system are the biochemical processes performed by the microorganisms.

The main objective of this work was to screen key state indicators that would allow to on-line monitor the performance of a HRAP treating UWW using a microalgae-bacteria consortium (in terms of biomass productivity, nutrient removal rate, photosynthetic efficiency and carbon dioxide biofixation). For this purpose, experiments were carried out using a 56 m^2 pilot-scale HRAP (working volume of 22 m^3), enabling the extrapolation of the observed results to industrial-scale processes. The pilot-scale HRAP was evaluated under highly variable conditions, *i.e.* during the start-up period. A statistical multivariate projection approach was followed for screening of the monitoring variables, which could be used for control and optimization purposes.

2. Materials and methods

2.1. Start-up of the HRAP and influent wastewater

No active inoculation of the HRAP was needed, implying that an initial natural selection of the predominant microorganisms occurred. This approach facilitates a potential industrial application of this technology.

Table 1 shows the main characteristics of the wastewater fed into the system. The synthetic UWW was weekly prepared according to Nopens et al. (2001). It was continually fed to the HRAP from a continuously-stirred tank with a volume of 500 L and refrigerated at 4 °C.

Table 1. Characteristics of the synthetic UWW

Parameter	Units	Mean ± SD
NH_4-N	mg $N \cdot L^{-1}$	17.3±8.1
N_T	mg $N \cdot L^{-1}$	45.5±24.2
PO_4-P	mg $P \cdot L^{-1}$	3.9±1.6
P_T	mg $P \cdot L^{-1}$	6.1±2.2
COD_T	$mg \cdot L^{-1}$	332±55
VSS	$mg \cdot L^{-1}$	89±24

UWW stands for urban wastewater, SD for standard deviation, NH_4-N for ammonium-N, N_T for total nitrogen, PO_4-P for phosphate-P, P_T for total phosphorous, COD_T for total chemical oxygen demand and VSS for volatile suspended solids

2.2. Description and operation of the pilot plant

This study was performed using a continuous HRAP with a working volume of 22 m^3. It had a liquid depth of 0.3 m and a solar irradiance area of approximately 73.4 m^2. The HRAP (located in the south of France, Lat. 43.156711, Long. 2.995075) was operated outdoors (*i.e.* under variable solar irradiance and T) at a hydraulic retention time (HRT) of 6 days. The reactor was continuously stirred by a paddlewheel. During the period of study, the daily average photosynthetic active radiation (PAR) was 433±113 (110-624) $\mu E \cdot m^{-2} \cdot s^{-1}$ (natural

light operation) and the culture T was 22±3 (16-27) ºC (ambient conditions). The pH varied freely according to variations in the concentration of carbon dioxide caused by the activity of microorganisms. The HRAP was run continuously for 36 days.

2.3. On-line and off-line monitoring of the pilot plant

Different on-line sensors were placed in the HRAP, which allowed continuous data acquisition. The on-line sensors used in this study were: (i) a pH-T transmitter (METTLER TOLEDO InPro® 4260 SG), (ii) a DO probe (METTLER TOLEDO InPro® 6800 G Amperometric Oxygen Sensor) and (iii) an irradiation sensor (Skye PAR Quantum Sensor) for measuring the PAR.

Besides the on-line process monitoring, samples were taken from the influent and the effluent streams to assess the performance of the biological processes. The concentrations of the following parameters were determined: total and soluble COD (COD_T and COD_S, respectively), N_T, P_T, inorganic nutrients (NH_4^+, NO_2^-, NO_3^- and PO_4^{3-}), total suspended solids (TSS) and volatile suspended solids (VSS). Additionally, optical density at 680 nm (OD_{680}) was also used for VSS estimation (VSS_{680}). Regarding the biomass composition, the copies per liter of 18S rDNA from chlorophyte and bacterial 16S rDNA were also determined.

2.4. Analytical methods and microbial analyses

The concentrations of COD_T, COD_S, N_T, P_T, TSS and VSS were analyzed according to Standard Methods (APHA, 2005). The concentrations of inorganic nutrients (NH_4^+, NO_2^-, NO_3^- and PO_4^{-3}) were measured by ion chromatography, as described in Capson-Tojo et al. (2017). The concentrations of free ammonia nitrogen (NH_3-N; FAN) were calculated using the Davies equation included in the geochemical equilibrium speciation model MINTEQA2 (Allison et al., 1991) via Visual MINTEQ (Gustafsson, 2012). The eukaryotic and prokaryotic cell numbers were estimated by quantitative polymerase chain reaction (qPCR). The presence of microalgal biomass was estimated targeting a partial sequence of 18S rDNA from

chlorophyte or bacillariophyte, whilst the total bacterial content was estimated using universal primers and probes for the 16S rDNA. A more extended description can be found in Turon et al. (2015).

2.5. HRAP performance monitoring

The process indicators used to monitor the performance of the microalgae-bacteria-based HRAP were the nitrogen removal rate (NRR) (g $N \cdot m^{-3} \cdot d^{-1}$), the biomass productivity per working volume (BP_V), the daily photosynthetic efficiency (PE), and the carbon dioxide biofixation (CO_{2BF}) (kg CO_2 per m^3 of treated water), which were calculated according to Eq. 1, Eq. 2, Eq. 3, and Eq. 4, respectively.

$$NRR = \frac{Q \cdot (N_i - N_e)}{V} \quad \text{(Eq. 1)}$$

$$BP_V = \frac{Q \cdot X_{VSS}}{V} \quad \text{(Eq. 2)}$$

Where Q is the treatment flow rate ($m^3 \cdot d^{-1}$), N_i is the influent nitrogen concentration (g $N \cdot m^{-3}$), N_e is the effluent nitrogen concentration (g $N \cdot m^{-3}$), V is the reaction volume (m^3), and X_{VSS} is the biomass concentration (g $VSS \cdot L^{-1}$).

$$PE\ (\%) = \frac{r_G \cdot H_B}{I \cdot S \cdot f} \cdot 100 \quad \text{(Eq. 3)}$$

$$CO_{2BF} = \frac{rG}{Y_{CO2} \cdot Q} \quad \text{(Eq. 4)}$$

Where r_G is the daily microalgae growth (kg $VSS \cdot d^{-1}$), H_B is the lower heating value of dry biomass (22,900 kJ·kg VSS^{-1}), I is the photosynthetic active radiation (µmol photons·$m^{-2} \cdot s^{-1}$), f is a conversion factor (18.78 kJ·s·µmol photons$^{-1} \cdot d^{-1}$), S is the surface of the open pond (m^2) and Y_{CO2} is the stoichiometric CO_2 capture for microalgae growth (0.52 kg VSS·kg CO_2^{-1}). For stoichiometric calculations of microalgae biomass composition, the chemical formula used in Viruela et al. (2018) was applied (*i.e.* $C_{106}H_{181}O_{45}N_{16}P$).

In order to assess the best key state indicators related to the performance of the microalgae-bacteria consortium (*i.e.* NRR, BP_V, PE, and CO_{2BF}), different variables were calculated from

on-line DO and pH measurements, using a microalgae kinetic model (Fernández et al., 2016). This allowed to confirm that the measured variables represented properly the physicochemical and biological processes occurring in the HRAP. At the same time, this process allowed obtaining variables that could lead to more precise predictions of the outputs/indicators (*i.e.* NRR, BP_V, PE, and CO_{2BF}) when compared to the raw DO or pH values.

Assuming non-inhibitory DO and pH conditions , Eq. 5 (see Fernández et al. (2016)) can be used to determine the photosynthesis rate (oxygen production rate; μ_{O_2}) as a function of I_i (a function of the average light irradiance (I_{av})) and a net, constant respiration/consumption rate (r_{O_2}).

$$\mu_{O_2} = \mu_{O_2 max} \cdot I_i - \alpha_s \cdot r_{O_2} \qquad \text{(Eq. 5)}$$

Where $\mu_{O_2 max}$ is the maximum oxygen production rate, and α_S is a distributed factor to account for the influence of shadows on the photosynthesis rate.

Four normalizing factors related to I_{av} (I_i) were considered in this work for representing different behaviors of microalgae in the HRAP. I_1 is a modified Monod-type factor reported by Fernández et al. (2016) (Eq. 6). I_2 is analogous to the duty cycle, which is the proportion of time at which microalgae are exposed to light (Fernández-Sevilla et al., 2018) (Eq. 7). I_3 is a Monod-type factor, where I_{av} acts as substrate, based on I_1 (Eq. 8). Lastly, I_4 is proposed based on I_3 where instead of k_i, PAR serves as semisaturation "constant" (Eq. 9).

$$I_1 = \frac{{I_{av}}^n}{k_i \cdot e^{m \cdot I_{av}} + {I_{av}}^n} \qquad \text{(Eq. 6)}$$

$$I_2 = \frac{I_{av}}{PAR} \qquad \text{(Eq. 7)}$$

$$I_3 = \frac{I_{av}}{I_{av} + k_i} \qquad \text{(Eq. 8)}$$

$$I_4 = \frac{I_{av}}{I_{av} + PAR} \qquad \text{(Eq. 9)}$$

Where n is a form exponent (1.045), k_i is a form parameter representing the optimum light

intensity (174 μE·m^{-2}·s^{-1}), m is a form parameter (0.0021), and PAR is the solar photosynthetically active radiation received by the HRAP (μmol·m^{-2}·s^{-1}).

The I_{av}, which integrates the light availability over the culture volume (Acién Fernández et al., 1997) can be calculated using Eq. 10.

$$I_{av} = \frac{I_0}{K_a \cdot C_b \cdot h} \cdot (1 - e^{-K_a \cdot C_b \cdot h}) \quad \text{(Eq. 10)}$$

Where I_0 is the solar irradiance on the pond surface (μE·m^{-2}·s^{-1}), K_a is an extinction coefficient (80 m^2·kg VSS^{-1}), C_b is the biomass concentration (kg·m^{-3}), and h is the liquid height (m).

In addition, the carbon dioxide kinetics (μ_{CO_2}) can be calculated from Eq. 11 considering a one-to-one molar ratio between oxygen and carbon dioxide (Fernández et al., 2016).

$$\mu_{CO_2} = -\mu_{O_2} \quad \text{(Eq. 11)}$$

Hence, Eq. 5 can be used for modelling the oxygen kinetics of the microalgae-bacteria consortia during daylight and night-time hours. Microalgae growth can be estimated by the first term of the right side of Eq. 5 when oxygen production during daylight hours is high enough to minimize the effect of algae respiration. In this study, average daily DO concentrations were above saturation conditions (saturations up to 200% were observed during daylight hours). It was therefore assumed that oxygen production during daylight hours was high enough to minimize the effect not only of microalgae respiration but also of heterotrophic and autotrophic bacteria consumption. On the other hand, microalgae respiration and bacteria growth can be estimated by the second term of the right side of Eq. 5 during night-time hours. Similarly, Eq. 11 can be used for modelling the carbon dioxide kinetics (pH dynamics).

Table 2 summarizes the different variables calculated in this study based on DO and pH measurements. The variables related to microalgae growth were also normalized to account

for the effect of I_{av} using Eq. 6 to Eq. 9. Specifically, the variables related to the first term of the right side of Eq. 5 were divided by the I_i function (considering the four I_{av} factors, I_1, I_2, I_3, and I_4) to approximate to the maximum growth rate of microalgae in the system. The resulting variables were noted as variable: I_i (*e.g.* DO_{AVE}:I_i). This normalization was not performed for those variables related to microalgae respiration and bacterial growth, since they represented the second term of the right side of Eq. 5. The process indicators NRR, BP_V, PE and CO_{2BF} were also normalized by the I_i function.

Table 2. Variables based on dissolved oxygen concentration (DO) and pH measurements

Variable acronym	Description [1]
DO_{AVE}	Dissolved oxygen average
DO_{MEDIAN}	Dissolved oxygen median
DO_{SD}	Dissolved oxygen standard deviation
DO_{MIN}	Minimum dissolved oxygen
DO_{MAX}	Maximum dissolved oxygen
DO_{RANGE}	Dissolved oxygen range
$DO_{MIN\ SLOPE1h}$	Minimum value of dissolved oxygen one-hour slope [2]
$DO_{MAX\ SLOPE1h}$	Maximum value of dissolved oxygen one-hour slope [3]
$DO_{AVE\ SLOPE1h}$	Absolute average of $DO_{MIN\ SLOPE1h}$ and $DO_{MAX\ SLOPE1h}$
$DO_{MIN\ SLOPE2h}$	Minimum value of dissolved oxygen two-hour slope [2]
$DO_{MAX\ SLOPE2h}$	Maximum value of dissolved oxygen two-hour slope [3]
$DO_{AVE\ SLOPE2h}$	Absolute average of $DO_{MIN\ SLOPE2h}$ and $DO_{MAX\ SLOPE2h}$
$DO_{INTEGRAL}$	Dissolved oxygen integral
$DO_{MAX:MIN\ ABS\ SLOPE1}$	Absolute value of $DO_{MAX\ SLOPE1h}$ to $DO_{MIN\ SLOPE1h}$ ratio
$DO_{MAX:MIN\ ABS\ SLOPE2h}$	Absolute value of $DO_{MAX\ SLOPE2h}$ to $DO_{MIN\ SLOPE2h}$ ratio
$DO_{SLOPE1h\ RANGE}$	Range of dissolved oxygen one-hour slope
$DO_{SLOPE2h\ RANGE}$	Range of dissolved oxygen two-hour slope
pH_{AVE}	pH average
pH_{MEDIAN}	pH median
pH_{MIN}	Minimum pH
pH_{MAX}	Maximum pH
$pH_{MAX:MIN}$	Maximum pH to minimum pH ratio

pH_{RANGE}	pH range
$pH_{MIN\ SLOPE1h}$	Minimum value of pH one-hour slope [2]
$pH_{MAX\ SLOPE1h}$	Maximum value of pH one-hour slope [3]
$pH_{AVE\ SLOPE1h}$	Absolute average of $pH_{MIN\ SLOPE1h}$ and $pH_{MAX\ SLOPE1h}$
$pH_{MIN\ SLOPE2h}$	Minimum value of pH two-hour slope [2]
$pH_{MAX\ SLOPE2h}$	Maximum value of pH two-hour slope [3]
$pH_{AVE\ SLOPE2h}$	Absolute average of $pH_{MIN\ SLOPE2h}$ and $pH_{MAX\ SLOPE2h}$
$pH_{INTEGRAL}$	pH integral
$pH_{MAX:MIN\ ABS\ SLOPE1}$	Absolute value of $pH_{MAX\ SLOPE1h}$ to $pH_{MIN\ SLOPE1h}$ ratio
$pH_{MAX:MIN\ ABS\ SLOPE2h}$	Absolute value of $pH_{MAX\ SLOPE2h}$ to $pH_{MIN\ SLOPE2h}$ ratio
$pH_{SLOPE1h\ RANGE}$	Range of pH one-hour slope
$pH_{SLOPE2h\ RANGE}$	Range of pH two-hour slope

1. Variables calculated within a time interval of one day
2. Minimum slopes were determined during night periods
3. Maximum slopes were determined during daylight periods

2.6. Multivariate projection analysis

Statistical analyses based on multivariate projection were performed to assess potential key state indicators based on pH and DO measurements affecting the HRAP performance. The mixOmics package (http://www.mixOmics.org) implemented in the R statistical software version 3.2.3 (http://www.R-project.org) was used for this purpose. Firstly, the set of calculated variables shown in Table 2 was statistically analyzed through principal component analysis (PCA) for screening and validation of potential key state indicators for real-time HRAP monitoring. PCA reduces the dimensionality of the data by creating uncorrelated artificial variables called principal components (PCs) that combine linearly the original variables, retaining as much information as possible (Wold et al., 1987). Particularly, the raw data set consisted of 34 variables with an observation each minute for the 36 days of HRAP operation. From this, daily average, minimum and maximum values analyzed (see Table 2). On the other hand, the relations between inputs (pH and DO variables), i.e. 34 variables, and the daily output process indicators (NRR, BP_V, PE and CO_{2BF}) were analyzed through partial least squares regression (PLSR). PLSR is a type of multivariate analysis (two-block predictive

PLS) for relating two data matrices, predictors (X) and responses (Y), by a linear multivariate model (Wold et al., 2001). By handling numerous and collinear X and Y values, PLSR allows investigating complex problems whilst analyzing data in a fairly realistic way.

3. Results and discussion

3.1. Performance of the HRAP

Figure 1A shows the evolution of the concentrations of COD and VSS and the OD in the mixed liquor during the experimental period. As it can be observed, the COD_S was rapidly consumed initially (days 1 to 5), which indicated a quick appearance and adaptation of heterotrophic bacteria in the system. Afterwards, the COD_S was 15±11 (5-25) $mg \cdot L^{-1}$ from day 10 until the end of the experimental period. This suggests that a stable community of heterotrophic bacteria was established in the system only after 10 days of operation. The stable values of the COD_T from day 10 to 18 corroborated this statement. During the first 10 days of operation, no significant photosynthetic activity was observed, with the number of 18S rDNA copies from chlorophyte remaining at low values (below 10^6 copies$\cdot mL^{-1}$; see Figure 1C). Relatively stable concentrations of heterotrophic bacteria were observed during the whole period (10^8-10^{10} copies 16S rDNA$\cdot mL^{-1}$). The values of the VSS, of 64±17 (45-109) $mg \cdot L^{-1}$ until day 18 (Figure 1A), also indicate that no significant variations in the biomass concentration existed during this initial operating stage. After day 18, a significant increase in the COD_T and VSS concentrations occurred, indicating the development of a microalgal community in the HRAP. This is in agreement with the increase in the 18S rDNA copies (chlorophyte) from day 11 until days 18-23, confirming the growth of microalgae. Therefore, a period of 18 days was needed in this study for the natural selection, development and adaptation of the most suitable phototrophic species within the cultivation medium and under the environmental and operating conditions applied. It is important to highlight that the

system was started-up without seed of bacterial or microalgal biomass, implying that the more suitable species were naturally selected.

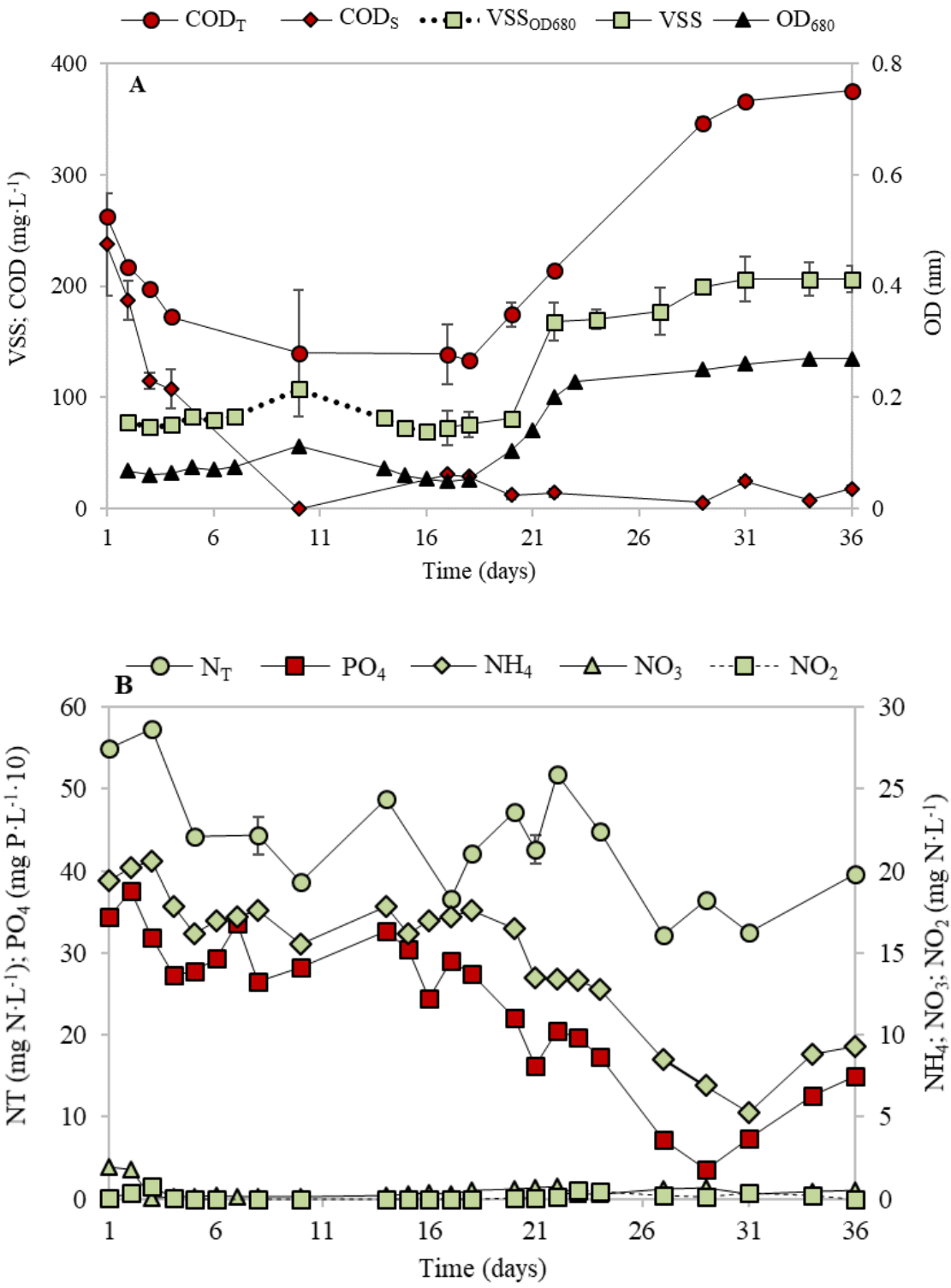

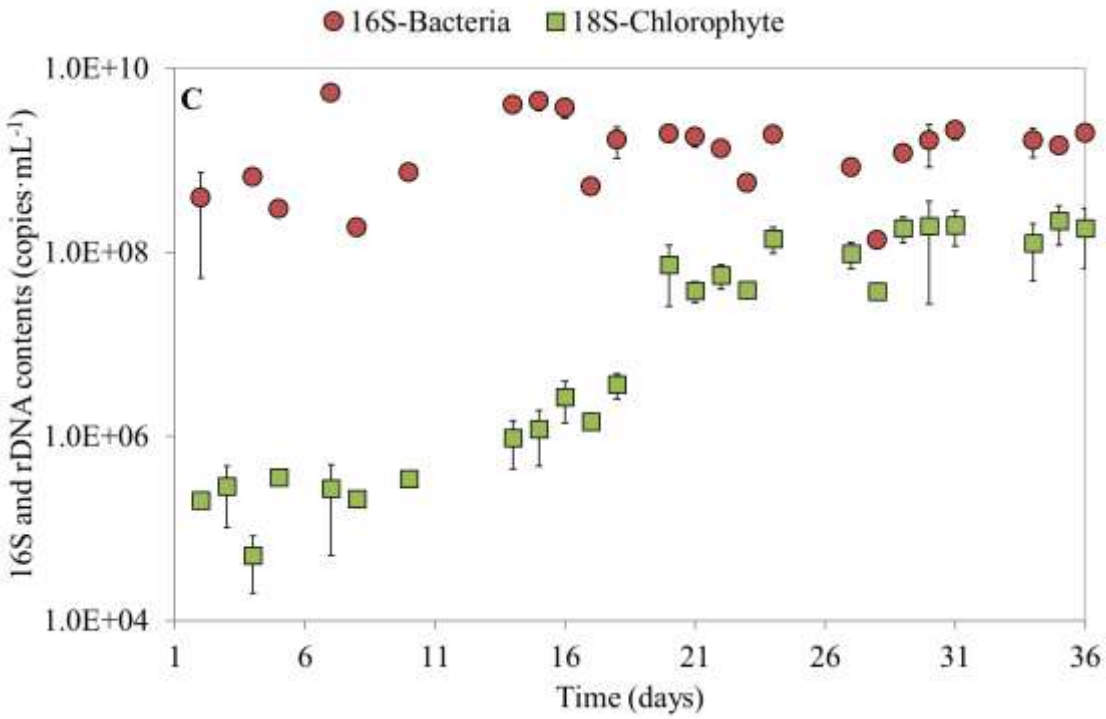

Figure 1. Evolution of (A) the total and soluble chemical oxygen demand (COD_T and COD_S), the measured and estimated volatile suspended solids (VSS and VSS_{OD680}) and the optical density at 680 nm (OD_{680}), (B) the total nitrogen concentration (N_T) and the concentrations of inorganic nutrients (PO_4^{3-}, NH_4^+, NO_3^- and NO_2^-) and (C) the contents of 16S rDNA copies (corresponding to bacteria) and 18S rDNA copies from chlorophyte (corresponding to microalgae)

Regarding the concentrations of different inorganic nutrients in the mixed liquor (*i.e.* PO_4^{3-}, NH_4^+, NO_3^- and NO_2^-), the results are shown in Figure 1B, together with the evolution of the concentration of N_T. As it could be expected from the previous results, the concentrations of NH_4-N and PO_4-P remained unchanged until day 18 due to the lack of algal growth, with values of 17.7±1.5 (20.5-15.5) mg NH_4-N·L^{-1} and 3.0±0.4 (3.7-2.4) mg PO_4-P·L^{-1}, respectively. Nevertheless, when microalgae started to grow (after day 18), the concentrations

of both nutrients started to decrease due to uptake by microalgae, reaching values of 7.8±1.7 (10.2-5.3) mg NH_4-N·L^{-1} and 0.9±0.5 (0.4-1.6) mg PO_4-P·L^{-1} when the process was fully functional (days 26-36). Considering that the European discharge limits in protected areas of treatment flows below 100,000 PE are 15 mg NH_4-N·L^{-1} and 2 mg PO_4-P·L^{-1} (European Council Directive 91/271/CEE), it can be concluded that, once a functional microalgae population was developed, the proposed system was able to treat the UWW efficiently in terms of nutrient content. Moving forwards, the N_T concentration showed a slight decrease from day 24 until the end of the experimental period (*i.e.* N_T decreased from an average of 44.8 mg N·L^{-1} between days 5-24 to 35.1 mg N·L^{-1} between days 25-36). This can be attributed to different factors: i) variations in the nitrogen loading rate to the system (influent N_T was 45.5±24.2 mg N·L^{-1}), ii) increased nitrification-denitrification rates, or iii) NH_3 loss due to volatilization at the relatively high pH values reached in the media during this period (above 8). The occurrence of nitrification-denitrification could not be verified by the nitrate and nitrite concentrations, which remained close to zero throughout the whole experimental period due to the switch between aerobic-anoxic conditions in the daylight and night-time hours (a maximum nitrate concentration of around 1 mg NO_3-N·L^{-1} was reached on day 21). Regarding NH_3 volatilization, Figure 2 shows the evolution of the total ammonia nitrogen concentration (sum of NH_4-N and FAN); TAN) during the experimental period. As it can be observed, the FAN to TAN ratio significantly increased with the pH of the culture media due to the phototrophic consumption of CO_2 by microalgae. Indeed, the FAN:TAN ratio increased with the pH. When the pH was above 8, the amount of FAN increased up to 25.8% of the TAN, suggesting a possible loss of NH_3 into the atmosphere. In absolute terms, nevertheless, FAN concentration reached maximum values of around 2 mg NH_3-N·L^{-1}. Thus, NH_3 volatilization cannot explain by itself the decrease in N_T observed in the system at the end of the experimental period. This suggests that other processes, such as variations in influent

nitrogen and/or nitrification-denitrification, occurred.

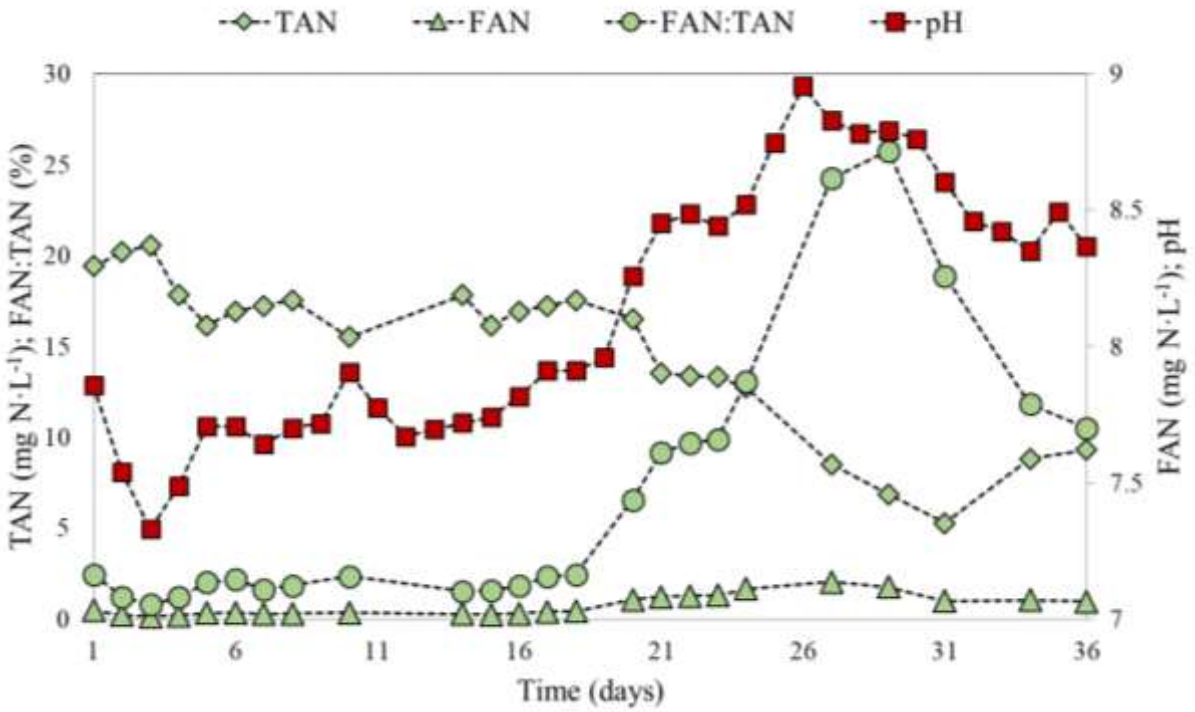

Figure 2. Evolution of the total ammonia nitrogen (TAN), the free ammonia nitrogen (FAN), the FAN to TAN ratio (FAN:TAN), and the pH of the media. All values represent daily averages

As key state indicators of the microbial performance of the HRAP, Figure 3A shows the evolution of the BP_V and NRR in the HRAP. As expected, both variables showed a significant increase around day 18, confirming the development of the microalgal community mentioned previously. After this point, the NRR experimented a sharp increase, reaching values up to 9 g $N \cdot m^{-3} \cdot d^{-1}$ and progressively decreasing from day 21 to day 26 until reaching nearly stable values around 4 g $N \cdot m^{-3} \cdot d^{-1}$. This behavior is consistent with the variables described previously (*i.e.* inorganic nutrient concentration and 18S rDNA copies content), confirming that the autotrophic growth of algae was directly responsible for the reduction in the

concentrations of the inorganic compounds measured. The higher NRR observed from days 18 to 23 can be attributed to a more efficient usage of the sunlight due to the lower initial biomass concentrations (*i.e.* lower biomass shading effect, allowing higher microalgal growth rates). In addition, the sharp decrease of the inorganic nutrient concentrations from day 21 to day 26 reduced their availability, which might have significantly reduced the microalgal growth rates. As previously, these results suggest that conditions of equilibrium were achieved after day 26, indicating a full start-up of the system. However, it must be mentioned that the biomass productivity experimented a slight increase around day 30, which could indicate that the minimum time for establishing adequate consortia between bacteria and microalgae could be of around one month of continuous operation. BP_V values during the steady-state period at the end of the experiment were around 30 g VSS·m^{-3}·d^{-1}, which are similar to those reported by Blanco et al. (2007) (40 g VSS·m^{-3}·d^{-1}).

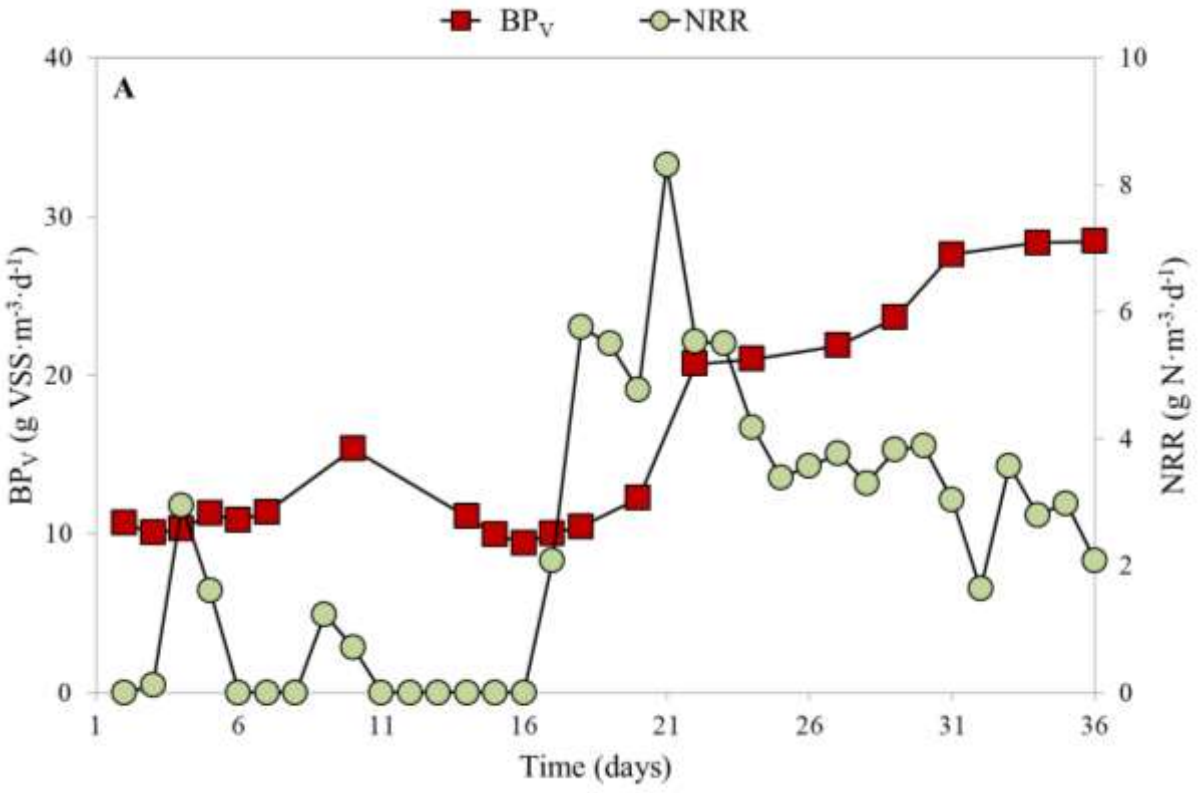

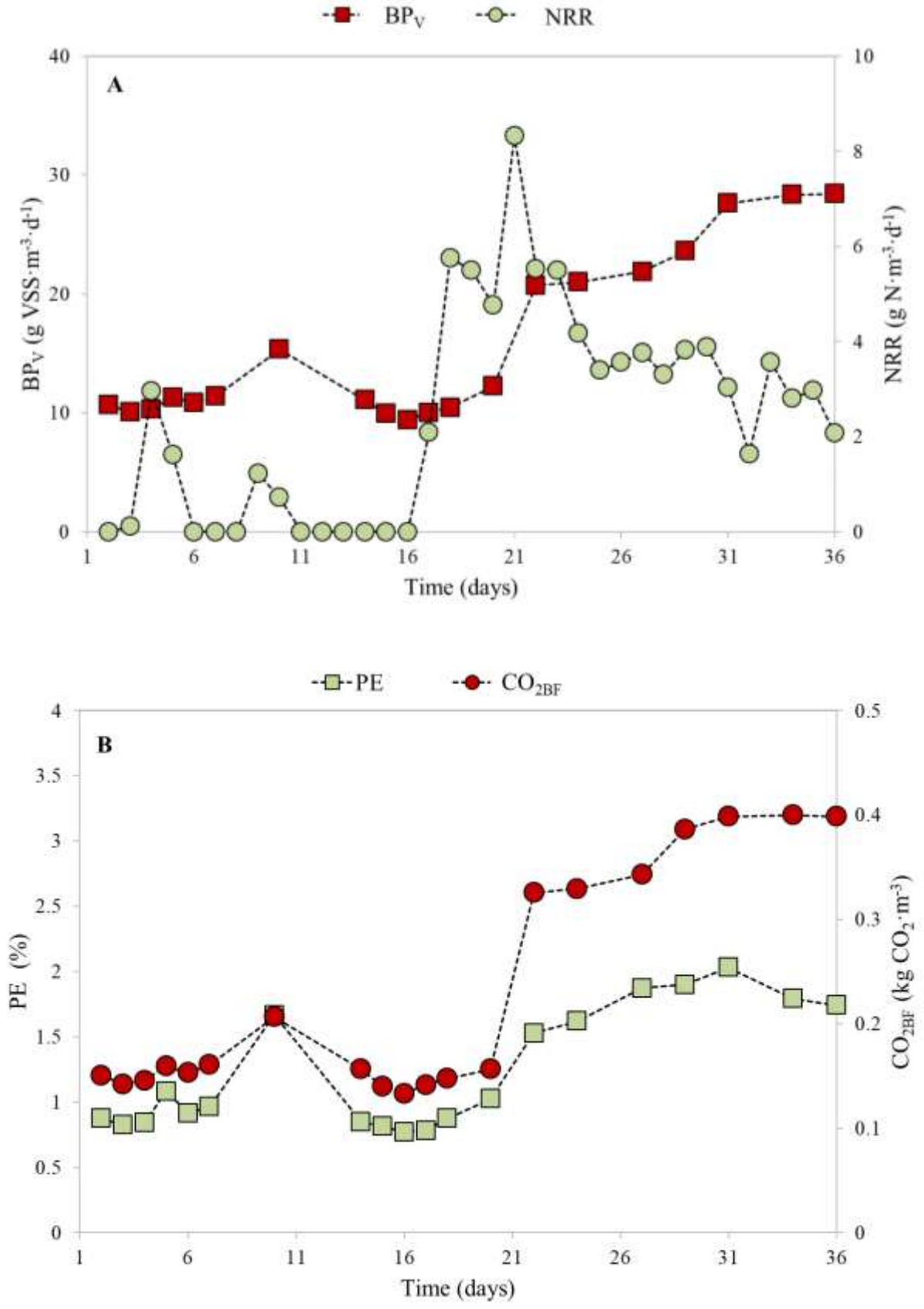

Figure 3. Evolution of (A) the biomass productivity per working volume (BP_V) and the

nitrogen removal rate (NRR) and (B) the photosynthetic efficiency (PE) and the carbon dioxide biofixation (CO_{2BF})

Figure 3B shows the evolution of the PE and the CO_{2BF} in the HRAP. As expected, both PE and CO_{2BF}, which depend on biomass productivity, showed a similar trend when compared to BP_V. PE yielded values of 1 % on day 30, which are below the theoretical maximum of 8-12 % (Romero Villegas et al., 2017). This suggests that further optimization of the process is possible. However, microalgae cultivation at industrial-scale, even at optimum conditions, rarely exceeds 1.5 to 2.0 % (Nwoba et al., 2019). In this respect, the light path and the light limitation of the outdoor configurations play a key role in light use efficiency. Several studies have assessed the effect of the culture depth (Arbib et al., 2017; Fernández et al., 2016) and how the light regime at which the microalgae are exposed to are far from the optimal values in outdoor raceway ponds (Barceló-Villalobos et al., 2019). Optimization of light use efficiency in system such as the one proposed in this study clearly deserve further research efforts. Regarding the CO_{2BF}, at the end of the experiment its value was around 0.28 kg CO_2 per m^3 of treated water (assuming $C_{106}H_{181}O_{45}N_{16}P$ as typical composition of algal biomass (Green et al., 1996). Viruela et al. (2018) reported maximum CO_{2BF} of 0.51 kg CO_2 per m^3 of treated water in a membrane photobioreactor (MPBR), similar to the results presented in this study, even if a less efficient microalgae cultivation system was used (HRAP). This reinforces the economic and environmental feasibility of this technology for UWW treatment.

3.2. Navigating on-line key state indicators

3.2.1. Results of the on-line monitoring of the process

As described previously, the DO and the pH were the variables measured on-line in this experiment. Figure 4 shows the evolution of the daily average DO concentrations and pH values in the mixed liquor throughout the experimental period. The DO concentrations

decreased sharply at the very beginning of the start-up period. This was caused by the initial activity of heterotrophic bacteria, corresponding to the initial COD consumption shown in Figure 1A. However, in accordance to the results presented in Figures 1-3, a sharp increase in the DO was observed between days 14 and 23, reaching values about 125 % of the DO saturation in water. During this period, the inorganic nutrient concentrations decreased and the chlorophyte concentrations increased. It was also during this period when the maximum NRR values were achieved. Therefore, it is clear that the DO increase was caused by the photosynthetic activity of microalgae. Regarding the pH, its value remained fairly constant until day 18 (around 7.7), when it increased up to almost 9 due to the consumption of CO_2, related again to the photosynthetic activity of the microalgae. Relatively stable values of around 8.4 were maintained after day 26, suggesting that an equilibrium of the carbon dioxide production-consumption had been reached.

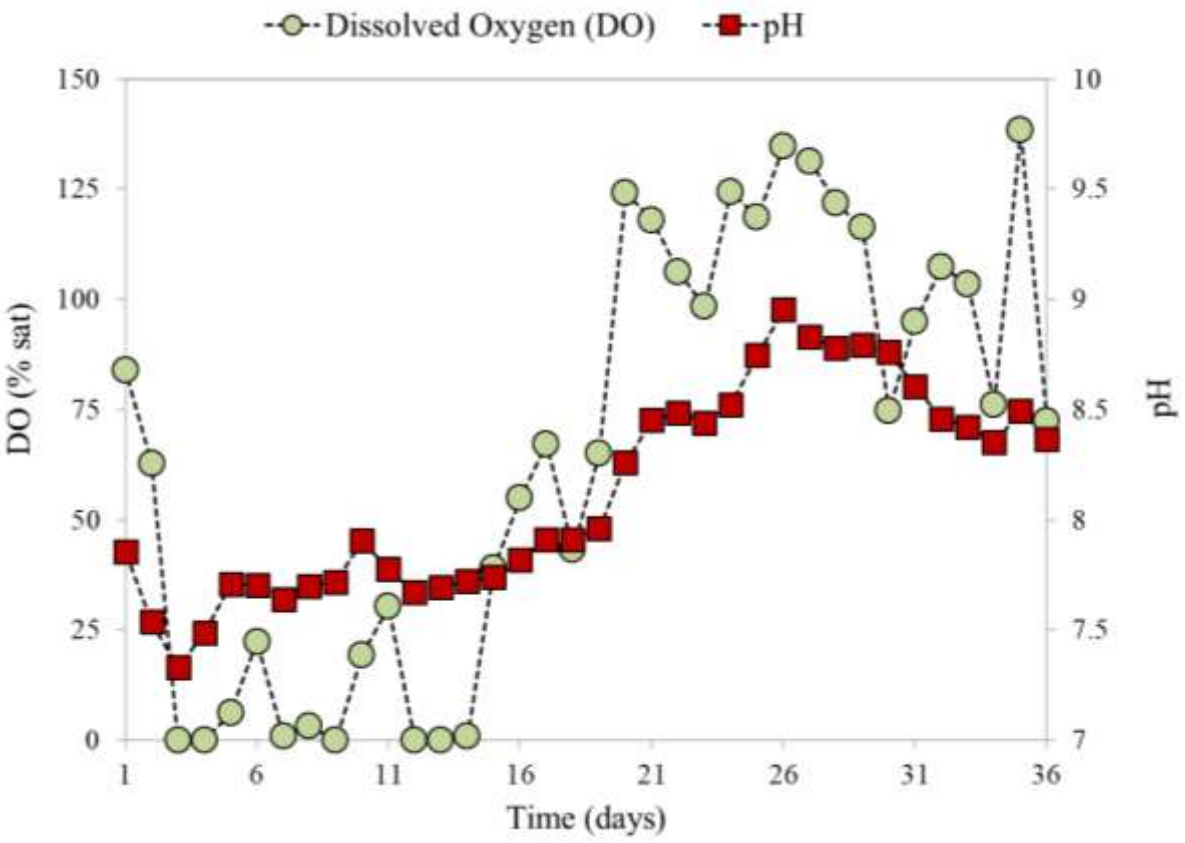

Figure 4. Evolution of the dissolved oxygen concentration (DO) and the pH in the mixed liquor throughout the experimental period

As expected, the evolution of the monitored variables (*i.e.* pH and DO) could easily explain the results presented above (Figure 1 to Figure 3). To obtain straight-forward results, statistical analyses were carried out to determine if these variables could be accurately used as predictors for key state indicators of the performance of microalgae-bacteria consortia.

3.2.2. Statistical identification of the key state indicators

Initially, PCA and PLSR analyses were carried out using all the available data (from whole experimental period). The obtained results are presented in Figure 5a and Figure 5b. Two PCs accounted for a cumulative explained variance of 75 %, indicating that the given results represent most of the contained information. The results of Figure 5a further confirm the

conclusions from the previous section, since two clusters were observed, which corresponded to data from day 1 to day 19 (bacteria community was predominant), and data from day 20 to day 36 (microalgae-bacteria community). These results confirm also the different behaviour of the HRAP plant with respect to the microalgal activity. Days 1 and 10 were considered outliers of the PCA. Day 1 corresponded to the start-up of the plant and day 10 was attributed to the activity of different microalgae species that were not successfully adapted to the operating and environmental conditions applied.

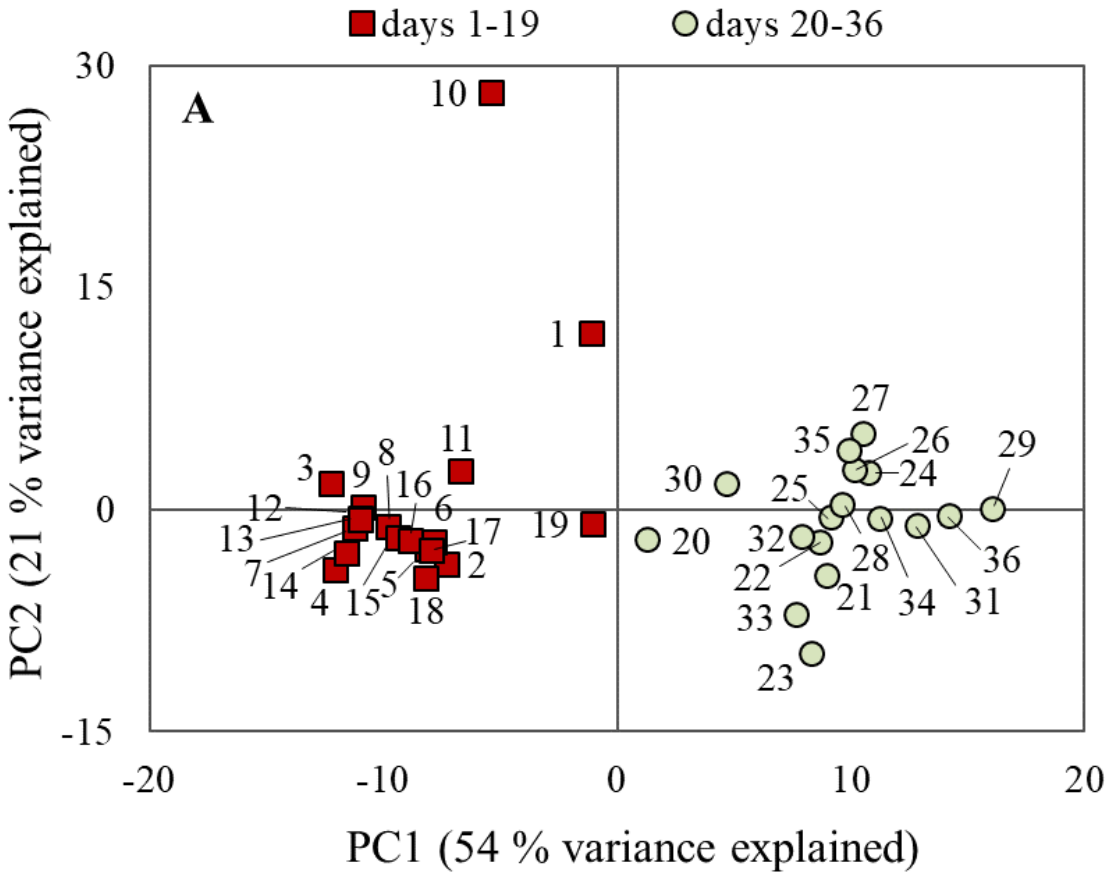

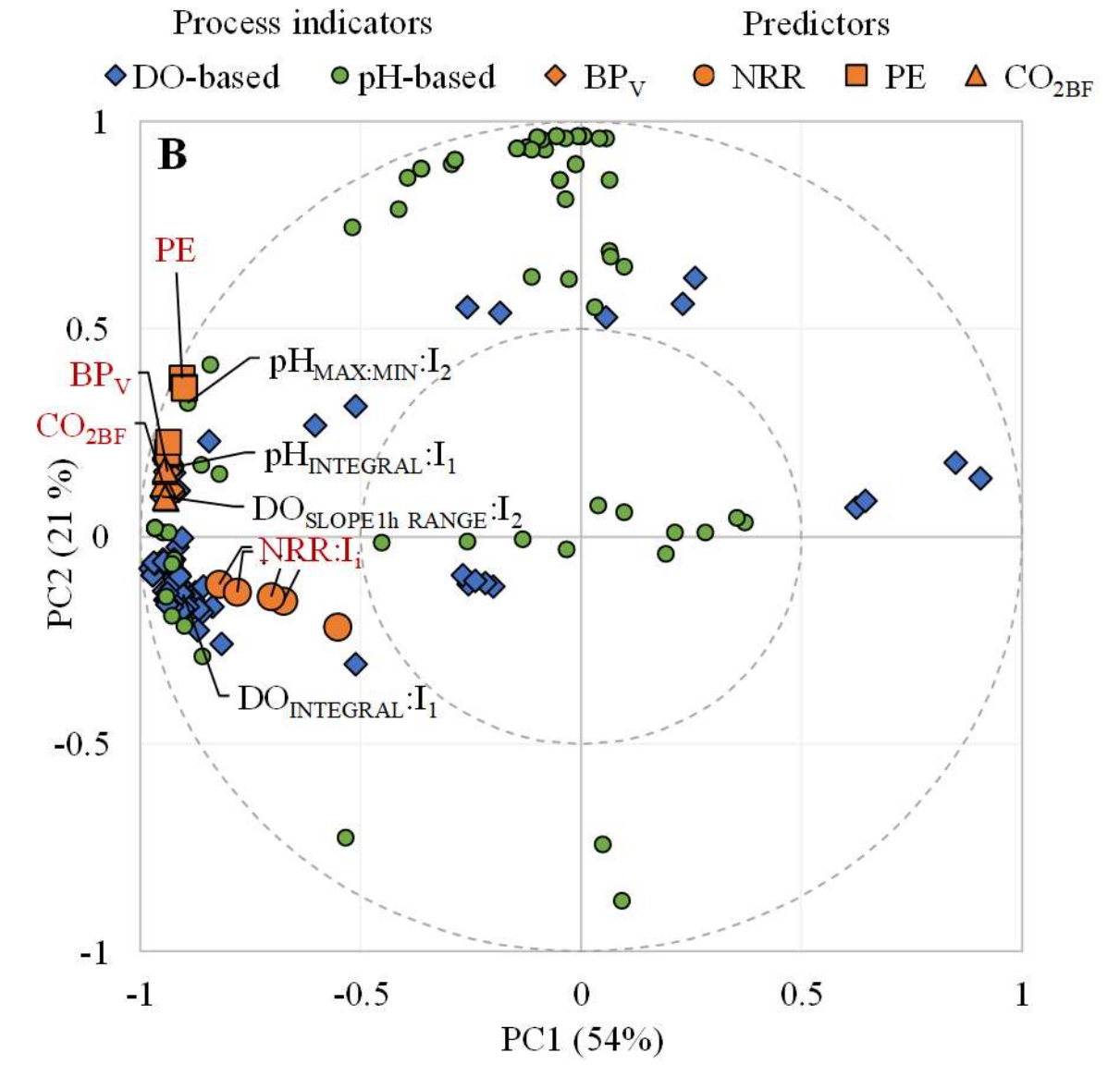

Figure 5. (A) Score plot for the first two components of the PCA model and (B) weight plot of the first two components of the PLSR model. DO stands for dissolved oxygen, BP_V for biomass productivity per working volume, NRR for nitrogen removal rate PE for photosynthetic efficiency and CO_{2BF} for carbon dioxide biofixation

Continuing with Figure 5B, the PLSR results show that the output process indicators BP_V, PE, and CO_{2BF} (and to a lesser extent NRR) are close to each other, since they are all directly related to the biomass activity. The clusters obtained between some parameters indicate that

they represented virtually the same information. For instance, the output process indicators (NRR:I_i, BP_V:I_i, PE:I_i, and CO_{2BF}:I_i), represent the same information with model I_1 and I_3 or the model I_2 and I_4. This implies that redundant values existed and therefore only one representative parameter of each cluster should be considered. In addition, non-standardized output process indicators (BP_V, PE, and CO_{2BF}; marked in red in Figure 5B) indicate similar information to the standardized ones except for NRR. In contrast, the best fitting of these output process indicators with the predictors was achieved when using I_i-normalized parameters based on pH and DO measurements (NRR:I_i marked in red in Figure 5B). Concerning the correlations between the predictors and the responses, the results of Figure 5B support the findings from the previous section due to the good correlations obtained. Specifically, stronger direct correlations were observed for the following pairs of parameters: $pH_{INTEGRAL}$:I_1 and BP_V, $DO_{SLOPE1h\,RANGE}$:I_2 and CO_{2BF}, $pH_{MAX:MIN}$:I_2 and PE, and $DO_{INTEGRAL}$:I_1 and NRR:I_i.

The $pH_{INTEGRAL}$:I_1 parameter represents the CO_2 availability in the media within the day derived from the microalgae-bacteria consortia performance. It is important to highlight that the biomass productivity was mainly related to microalgae growth, confirmed by particle size distribution analysis (data not shown). Thus, at higher concentrations of CO_2 available, higher microalgal activities are expected (with concomitant higher biomass productivities). The $DO_{SLOPE1h\,RANGE}$:I_2 parameter represents the O_2 availability in the media within the day. The oxygen production indeed derives from the photosynthetic activity, which is directly correlated to CO_2 biofixation. The $pH_{MAX:MIN}$:I_2 parameter represents microalgae growth rate versus the respiration rate of the microalgae. This respiration rate can be regarded as an indirect indicator of the maximum capacity of the system, since this process was not limited by the operating conditions. Hence, higher microalgae growth efficiencies (represented by $pH_{MAX:MIN}$:I_2) correspond to higher photosynthetic efficiencies. The $DO_{INTEGRAL}$:I_1 parameter

also represents the O_2 availability in the media within a day. At higher DO production rates, higher nitrogen uptake rates by microalgae and higher nitrification capacities of the system can be expected. These results prove that pH and DO-derived variables can accurately be used to predict the general performance of the HRAP.

Nevertheless, since two representative sets of parameters were observed in Figure 5a (days 1-19 and days 20-36), two PLSR models (one per data set) were conducted aiming at determining which variables predicted more accurately the process outputs depending on the behavior of the system (Figure 6). Similar to Figure 5B, Figure 6A (showing the data set corresponding to days 1-19) shows that process indicators BP_V, PE, and CO_{2BF} are nearby in the PLS plot. NRR was not significantly correlated to any other variable since neither significant microalgal activity nor nitrification were observed until day 14. In this case, the PLSR results show a strong correlation between the outputs and the predictor $pH_{MAX:MIN}$:I_2. As commented before, this parameter is related to the microalgal activity. Thus, this variable can be useful for assessing the initial dynamics of microalgae growth (days 14-19; see Figure 3), representing precisely BP_V, CO_{2BF} and PE during this period. NRR could be predicted by different DO-based variables, such as DO_{MIN}:I_1, suggesting that this parameter can be used for monitoring the initial performance of the system. This is a logical output, as NRR was mainly determined at this point by bacterial growth, which were responsible for oxygen consumption.

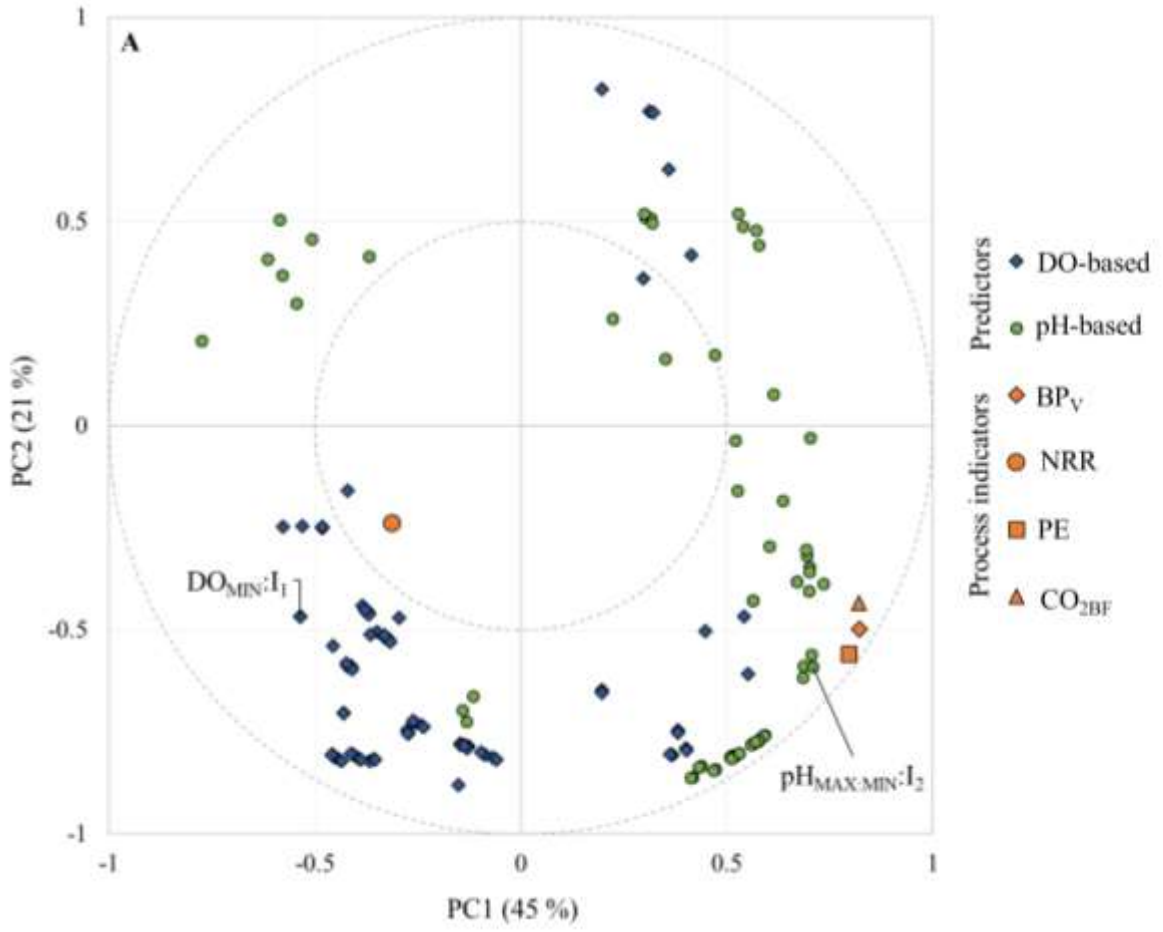
A
PC2 (21 %)
PC1 (45 %)
1
0.5
0
-0.5
-1
-1
-0.5
0
0.5
1
DO_{MIN}:I_1
$pH_{MAX-MIN}$:I_2
Predictors
DO-based
pH-based
Process indicators
BP_V
NRR
PE
CO_{2BF}

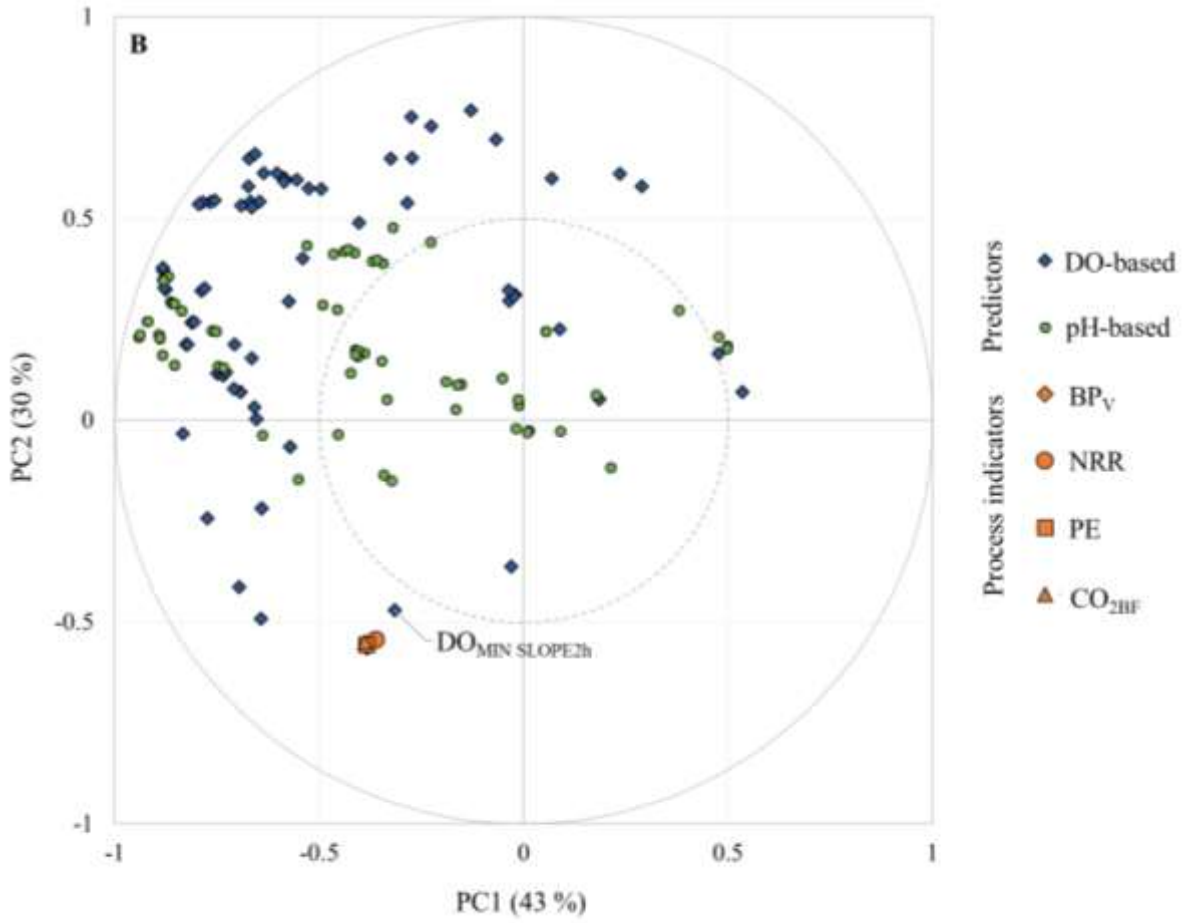

Figure 6. Weight plot (correlation circles) of the first two components of the PLSR model for (A) days 1-19, and (B) days 20-36. DO stands for dissolved oxygen, BP_V for biomass productivity per working volume, NRR for nitrogen removal rate PE for photosynthetic efficiency and CO_{2BF} for carbon dioxide biofixation

Figure 6B shows the results from the PLSR model conducted with data during the period of stable operation of plant (days 20-36). Indeed, all the responses evaluated in the PLSR model resulted in the same location in the PLS plot, indicating a fully developed consortium. The direct correlation of NRR and the other process indicators further confirms the dominant microalgal activity. In this case, the predictor that better correlates with the responses is the variable $DO_{MIN\ SLOPE2h}$. This variable represents the consumption of oxygen by respiration of

microalgae and by growth of heterotopic microorganisms, which are the main processes occurring in a fully developed microalgae-bacteria consortia during the night (when the minimum slopes were determined).

These results suggest that both pH and DO can be accurately used for a proper monitoring of the microbial processes occurring in HRAPs treating UWW by microalgae-bacteria consortia. They could also be applied potentially for the prediction of the performances that can be achieved, applying simple regression analysis. Other than being in agreement with different studies performed with microalgae in HRAPs (Galès et al., 2019; Havlik et al., 2013), the conclusions from this work also agree with the results presented in Foladori et al. (2018), another study dealing with monitoring of microalgae-bacteria consortia for WWT. In their research, the DO, the pH and the ORP were monitored in real-time using on-line probes installed in a sequential PBR, revealing that the evolution of the WWT process could be followed by measuring the aforementioned parameters. The real-time on-line monitoring of both the pH and the DO offers an easily-applicable option for monitoring, control and optimize industrial-scale HRAPs, using affordable probes already available in the market. The normalized variables can also provide accurate indications of the performance of the HRAP when compared to an optimal behavior, serving as markers for disturbances in the system. This approach has a great potential, not only to monitor and control the proper operation of the proposed WWT system, but also to optimize the achieved performances and to increase the understanding of the underlying processes when coupling monitoring with novel mathematical models, such as the one presented in Solimeno et al. (2017b).

4. Conclusions

A stable bacterial community was stablished after 10 days. It took around 19 days to develop a microalgal community able to uptake nutrients effectively. After 26 days, the HRAPs was

fully functional, meeting the European discharge limits. Variations in the biomass productivities in days 26-30 suggest that the minimum time required for establishing a performant microbial population was around one month. The statistical analyses show that pH-based and DO-based variables can represent accurately the biochemical processes taking place. Both the pH and the DO could also be used to accurately describe the HRAP performance. This represents an affordable, easily-implemented option for on-line monitoring, control and optimize industrial-scale processes.

Acknowledgements

The authors acknowledge the financial support of the French National Research Agency (ANR) for the "Phycover" project (project ANR-14-CE04-0011), the Spanish Ministry of Economy and Competitiveness (MINECO, Projects CTM2014-54980-C2-1-R and CTM2014-54980-C2-2-R) jointly with the European Regional Development Fund (ERDF), and the European Climate KIC association for the "MAB 2.0" project (APIN0057_2015-3.6-230_P066-05). Ángel Robles would also like to acknowledge the financial aid received from Generalitat Valenciana via a VALi+d post-doctoral grant (APOSTD/2014/049). Gabriel Capson-Tojo is grateful to the Xunta de Galicia for his postdoctoral fellowship (ED481B-2018/017).

References

Acién Fernández, F.G., García Camacho, F., Sánchez Pérez, J.A., Fernández Sevilla, J.M., Molina Grima, E., 1997. A model for light distribution and average solar irradiance inside outdoor tubular photobioreactors for the microalgal mass culture. Biotechnol. Bioeng. 55, 701–714. https://doi.org/10.1002/(SICI)1097-0290(19970905)55:5<701::AID-BIT1>3.0.CO;2-F

Allison, J.D., Brown, D.S., Novo-Gradac, K.J., 1991. MINTEQA2/ PRODEFA2, A Geochemical Assessment Model for Environmental Systems: Version 3.0. EPA/600/3-91/021, USEPA, Washington, DC.

APHA, 2005. Standard Methods for the Examination of Water and Wastewater. American Public Health Association, Washington, DC.

Arbib, Z., de Godos, I., Ruiz, J., Perales, J.A., 2017. Optimization of pilot high rate algal ponds for simultaneous nutrient removal and lipids production. Sci. Total Environ. 589, 66–72. https://doi.org/10.1016/j.scitotenv.2017.02.206

Arbib, Z., Ruiz, J., álvarez-Díaz, P., Garrido-Pérez, C., Barragan, J., Perales, J.A., 2013. Long term outdoor operation of a tubular airlift pilot photobioreactor and a high rate algal pond as tertiary treatment of urban wastewater. Ecol. Eng. 52, 143–153. https://doi.org/10.1016/j.ecoleng.2012.12.089

Barceló-Villalobos, M., Fernández-del Olmo, P., Guzmán, J.L., Fernández-Sevilla, J.M., Acién Fernández, F.G., 2019. Evaluation of photosynthetic light integration by microalgae in a pilot-scale raceway reactor. Bioresour. Technol. 280, 404–411. https://doi.org/10.1016/j.biortech.2019.02.032

Berenguel, M., Rodríguez, F., Acién, F.G., García, J.L., 2004. Model predictive control of pH in tubular photobioreactors. J. Process Control 14, 377–387. https://doi.org/10.1016/j.jprocont.2003.07.001

Blanco, A.M., Moreno, J., Del Campo, J.A., Rivas, J., Guerrero, M.G., 2007. Outdoor cultivation of lutein-rich cells of Muriellopsis sp. in open ponds. Appl. Microbiol. Biotechnol. 73, 1259–1266. https://doi.org/10.1007/s00253-006-0598-9

Boelee, N.C., Temmink, H., Janssen, M., Buisman, C.J.N., Wijffels, R.H., 2011. Nitrogen and phosphorus removal from municipal wastewater effluent using microalgal biofilms. Water Res. 45, 5925–5933. https://doi.org/10.1016/j.watres.2011.08.044

Capson-Tojo, G., Rouez, M., Crest, M., Trably, E., Steyer, J., Bernet, N., Delgenes, J., Escudié, R., 2017. Kinetic study of dry anaerobic co-digestion of food waste and cardboard for methane production. Waste Manag. 69, 470–479. https://doi.org/10.1016/j.wasman.2017.09.002

Craggs, R.J., Heubeck, S., Lundquist, T.J., Benemann, J.R., 2011. Algal biofuels from wastewater treatment high rate algal ponds. Water Sci. Technol. 63, 660 LP – 665.

Dalrymple, O.K., Halfhide, T., Udom, I., Gilles, B., Wolan, J., Zhang, Q., Ergas, S., 2013. Wastewater use in algae production for generation of renewable resources : a review and preliminary results. Aquat. Biosyst. 9, 1–11.

De Andrade, G.A., Berenguel, M., Guzmán, J.L., Pagano, D.J., Acién, F.G., 2016. Optimization of biomass production in outdoor tubular photobioreactors. J. Process Control 37, 58–69. https://doi.org/10.1016/j.jprocont.2015.10.001

Esposito, S., Cafiero, A., Giannino, F., Mazzoleni, S., Diano, M.M., 2017. A Monitoring, Modeling and Decision Support System (DSS) for a Microalgae Production Plant based on Internet of Things Structure. Procedia Comput. Sci. 113, 519–524. https://doi.org/10.1016/j.procs.2017.08.316

Faried, M., Samer, M., Abdelsalam, E., Yousef, R.S., Attia, Y.A., Ali, A.S., 2017. Biodiesel production from microalgae: Processes, technologies and recent advancements. Renew. Sustain. Energy Rev. 79, 893–913. https://doi.org/10.1016/j.rser.2017.05.199

Fernández-Sevilla, J.M., Brindley, C., Jiménez-Ruíz, N., Acién, F.G., 2018. A simple equation to quantify the effect of frequency of light/dark cycles on the photosynthetic

response of microalgae under intermittent light. Algal Res. 35, 479–487. https://doi.org/10.1016/j.algal.2018.09.026

Fernández, I., Acién, F.G., Guzmán, J.L., Berenguel, M., Mendoza, J.L., 2016. Dynamic model of an industrial raceway reactor for microalgae production. Algal Res. 17, 67–78. https://doi.org/10.1016/j.algal.2016.04.021

Foladori, P., Petrini, S., Andreottola, G., 2018. Evolution of real municipal wastewater treatment in photobioreactors and microalgae-bacteria consortia using real-time parameters. Chem. Eng. J. 345, 507–516. https://doi.org/10.1016/j.cej.2018.03.178

Galès, A., Bonnafous, A., Carré, C., Jauzein, V., Lanouguère, E., Le, E., Pinoit, J., Poullain, C., Roques, C., Sialve, B., Simier, M., Steyer, J., Fouilland, E., 2019. Importance of ecological interactions during wastewater treatment using High Rate Algal Ponds under different temperate climates. Algal Res. 40, 101508. https://doi.org/10.1016/j.algal.2019.101508

González-Camejo, J., Jiménez-Benítez, A., Ruano, M. V., Robles, A., Barat, R., Ferrer, J., 2019. Optimising an outdoor membrane photobioreactor for tertiary sewage treatment. J. Environ. Manage. 245, 76–85. https://doi.org/10.1016/j.jenvman.2019.05.010

González-Camejo, J., Serna-García, R., Viruela, A., Pachés, M., Durán, F., Robles, A., Ruano, M. V., Barat, R., Seco, A., 2017. Short and long-term experiments on the effect of sulphide on microalgae cultivation in tertiary sewage treatment. Bioresour. Technol. 244, 15–22. https://doi.org/10.1016/j.biortech.2017.07.126

Green, F.B., Bernstone, L.S., Lundquist, T.J., Oswald, W.J., 1996. Advanced integrated wastewater pond systems for nitrogen removal. Water Sci. Technol. 33, 207–217. https://doi.org/10.1016/0273-1223(96)00356-3

Gustafsson, J.P., 2012. Visual MINTEQ [WWW Document]. URL http://vminteq.lwr.kth.se/download/

Havlik, I., Lindner, P., Scheper, T., Reardon, K.F., 2013. On-line monitoring of large cultivations of microalgae and cyanobacteria. Trends Biotechnol. 31, 406–414. https://doi.org/10.1016/j.tibtech.2013.04.005

Kumar, K., Mishra, S.K., Shrivastav, A., Park, M.S., Yang, J.W., 2015. Recent trends in the mass cultivation of algae in raceway ponds. Renew. Sustain. Energy Rev. 51, 875–885. https://doi.org/10.1016/j.rser.2015.06.033

Lardon, L., Helias, A., Sialve, B., Steyer, J.-P., Bernard, O., 2009. Life-Cycle Assessment of Biodiesel Production from Microalgae. Enviromental Sci. Technol. 43, 6475–6481.

Larsdotter, K., 2006. Wastewater treatment with microalgae – a literature review 62, 31–38.

Liu, J., Wu, Y., Wu, C., Muylaert, K., Vyverman, W., Yu, H.Q., Muñoz, R., Rittmann, B., 2017. Advanced nutrient removal from surface water by a consortium of attached microalgae and bacteria: A review. Bioresour. Technol. 241, 1127–1137. https://doi.org/10.1016/j.biortech.2017.06.054

Luo, Y., Le-Clech, P., Henderson, R.K., 2017. Simultaneous microalgae cultivation and wastewater treatment in submerged membrane photobioreactors: A review. Algal Res. 24, 425–437. https://doi.org/10.1016/J.ALGAL.2016.10.026

Mata, T.M., Martins, A.A., Caetano, N.S., 2010. Microalgae for biodiesel production and other applications: A review. Renew. Sustain. Energy Rev. 14, 217–232.

https://doi.org/10.1016/J.RSER.2009.07.020

Mohd Udaiyappan, A.F., Abu Hasan, H., Takriff, M.S., Sheikh Abdullah, S.R., 2017. A review of the potentials, challenges and current status of microalgae biomass applications in industrial wastewater treatment. J. Water Process Eng. 20, 8–21. https://doi.org/10.1016/j.jwpe.2017.09.006

Muñoz-Tamayo, R., Mairet, F., Bernard, O., 2013. Optimizing microalgal production in raceway systems. Biotechnol. Prog. 29, 543–552. https://doi.org/10.1002/btpr.1699

Nopens, I., Capalozza, C., Vanrolleghem, P.A., 2001. Stability analysis of a synthetic municipal wastewater. Gent. https://doi.org/10.1017/CBO9781107415324.004

Novoveská, L., Zapata, A.K.M., Zabolotney, J.B., Atwood, M.C., Sundstrom, E.R., 2016. Optimizing microalgae cultivation and wastewater treatment in large-scale offshore photobioreactors. Algal Res. 18, 86–94. https://doi.org/10.1016/j.algal.2016.05.033

Nwoba, E.G., Parlevliet, D.A., Laird, D.W., Alameh, K., Moheimani, N.R., 2019. Light management technologies for increasing algal photobioreactor efficiency. Algal Res. 39, 101433. https://doi.org/10.1016/j.algal.2019.101433

Park, J.B.K., Craggs, R.J., Shilton, A.N., 2011. Wastewater treatment high rate algal ponds for biofuel production. Bioresour. Technol. 102, 35–42. https://doi.org/10.1016/J.BIORTECH.2010.06.158

Romero Villegas, G.I., Fiamengo, M., Acién Fernández, F.G., Molina Grima, E., 2017. Outdoor production of microalgae biomass at pilot-scale in seawater using centrate as the nutrient source. Algal Res. 25, 538–548. https://doi.org/10.1016/j.algal.2017.06.016

Solimeno, A., Gabriel, F., García, J., 2017a. Mechanistic model for design, analysis, operation and control of microalgae cultures: Calibration and application to tubular photobioreactors. Algal Res. 21, 236–246. https://doi.org/10.1016/j.algal.2016.11.023

Solimeno, A., Parker, L., Lundquist, T., García, J., 2017b. Integral microalgae-bacteria model (BIO_ALGAE): Application to wastewater high rate algal ponds. Sci. Total Environ. 601–602, 646–657. https://doi.org/10.1016/j.scitotenv.2017.05.215

Tran, K.C., Mendoza Martin, J.L., Heaven, S., Banks, C.J., Acien Fernandez, F.G., Molina Grima, E., 2014. Cultivation and anaerobic digestion of Scenedesmus spp. grown in a pilot-scale open raceway. Algal Res. 5, 95–102. https://doi.org/10.1016/j.algal.2014.06.001

Turon, V., Trably, E., Fayet, A., Fouilland, E., Steyer, J.P., 2015. Raw dark fermentation effluent to support heterotrophic microalgae growth: Microalgae successfully outcompete bacteria for acetate. Algal Res. 12, 119–125. https://doi.org/10.1016/j.algal.2015.08.011

Uggetti, E., Sialve, B., Latrille, E., Steyer, J.P., 2014. Anaerobic digestate as substrate for microalgae culture: The role of ammonium concentration on the microalgae productivity. Bioresour. Technol. 152, 437–443. https://doi.org/10.1016/j.biortech.2013.11.036

Ugwu, C.U., Aoyagi, H., Uchiyama, H., 2008. Photobioreactors for mass cultivation of algae. Bioresour. Technol. 99, 4021–4028. https://doi.org/10.1016/j.biortech.2007.01.046

Vasumathi, K.K., Premalatha, M., Subramanian, P., 2012. Parameters influencing the design of photobioreactor for the growth of microalgae. Renew. Sustain. Energy Rev. 16, 5443–5450. https://doi.org/10.1016/J.RSER.2012.06.013

Viruela, A., Robles, Á., Durán, F., Ruano, M.V., Barat, R., Ferrer, J., Seco, A., 2018. Performance of an outdoor membrane photobioreactor for resource recovery from anaerobically treated sewage. J. Clean. Prod. 178, 665–674. https://doi.org/10.1016/j.jclepro.2017.12.223

Wang, Y., Guo, W., Yen, H.W., Ho, S.H., Lo, Y.C., Cheng, C.L., Ren, N., Chang, J.S., 2015. Cultivation of Chlorella vulgaris JSC-6 with swine wastewater for simultaneous nutrient/COD removal and carbohydrate production. Bioresour. Technol. 198, 619–625. https://doi.org/10.1016/j.biortech.2015.09.067

Wang, Y., Ho, S.-H., Cheng, C.-L., Guo, W.-Q., Nagarajan, D., Ren, N.-Q., Lee, D.-J., Chang, J.-S., 2016. Perspectives on the feasibility of using microalgae for industrial wastewater treatment. Bioresour. Technol. 222, 485–497. https://doi.org/10.1016/J.BIORTECH.2016.09.106

Wold, S., Esbensen, K., Geladi, P., 1987. Principal component analysis. Chemom. Intell. Lab. Syst. 2, 37–52.

Wold, S., Sjöström, M., Eriksson, L., 2001. PLS-regression: A basic tool of chemometrics. Chemom. Intell. Lab. Syst. 58, 109–130. https://doi.org/10.1016/S0169-7439(01)00155-1

Figure and table captions

Figure 1. Evolution of (A) the total and soluble chemical oxygen demand (COD_T and COD_S), the measured and estimated volatile suspended solids (VSS and VSS_{OD680}) and the optical density at 680 nm (OD_{680}), (B) the total nitrogen concentration (N_T) and the concentrations of inorganic nutrients (PO_4^{3-}, NH_4^+, NO_3^- and NO_2^-) and (C) the contents of 16S rDNA copies (corresponding to bacteria) and 18S rDNA copies from chlorophyte (corresponding to microalgae)

Figure 2. Evolution of the total ammonia nitrogen (TAN), the free ammonia nitrogen (FAN), the FAN to TAN ratio (FAN:TAN), and the pH of the media. All values represent daily averages

Figure 3. Evolution of (A) the biomass productivity per working volume (BP_V) and the nitrogen removal rate (NRR) and (B) the photosynthetic efficiency (PE) and the carbon dioxide biofixation (CO_{2BF})

Figure 4. Evolution of the dissolved oxygen concentration (DO) and the pH in the mixed liquor throughout the experimental period

Figure 5. (A) Score plot for the first two components of the PCA model and (B) weight plot of the first two components of the PLSR model. DO stands for dissolved oxygen, BP_V for biomass productivity per working volume, NRR for nitrogen removal rate PE for photosynthetic efficiency and CO_{2BF} for carbon dioxide biofixation

Figure 6. Weight plot (correlation circles) of the first two components of the PLSR model for (A) days 1-19, and (B) days 20-36. DO stands for dissolved oxygen, BP_V for biomass productivity per working volume, NRR for nitrogen removal rate PE for photosynthetic efficiency and CO_{2BF} for carbon dioxide biofixation

Table 1. Characteristics of the synthetic UWW

Table 2. Variables based on dissolved oxygen concentration (DO) and pH measurements